

Disguise without Disruption: Utility-Preserving Face De-Identification

Zikui Cai¹*, Zhongpai Gao², Benjamin Planche², Meng Zheng³,
Terrence Chen², M. Salman Asif¹, Ziyang Wu²

¹University of California, Riverside, CA {zca1032, sasif}@ucr.edu
²United Imaging Intelligence, Burlington, MA {first.last}@uii-ai.com
³Rensselaer Polytechnic Institute, Troy, NY zhengm5@rpi.edu

Abstract

With the rise of cameras and smart sensors, humanity generates an exponential amount of data. This valuable information, including underrepresented cases like AI in medical settings, can fuel new deep-learning tools. However, data scientists must prioritize ensuring privacy for individuals in these untapped datasets, especially for images or videos with faces, which are prime targets for identification methods. Proposed solutions to de-identify such images often compromise non-identifying facial attributes relevant to downstream tasks. In this paper, we introduce *Disguise*, a novel algorithm that seamlessly de-identifies facial images while ensuring the usability of the modified data. Unlike previous approaches, our solution is firmly grounded in the domains of differential privacy and ensemble-learning research. Our method involves extracting and substituting depicted identities with synthetic ones, generated using variational mechanisms to maximize obfuscation and non-invertibility. Additionally, we leverage supervision from a mixture-of-experts to disentangle and preserve other utility attributes. We extensively evaluate our method using multiple datasets, demonstrating a higher de-identification rate and superior consistency compared to prior approaches in various downstream tasks.

Introduction

Global privacy laws safeguard personal data, including regulations like GDPR (Voigt and Von dem Bussche 2017) in Europe, HIPAA (HIP 2003) and CCPA (CCP 2018) in the US, and PIPL (PIP 2021) in China. Particularly stringent for medical information and data from medical settings, these rules tightly control storage and distribution of patient images to ensure confidentiality. Yet, this data holds valuable potential, such as automating medical procedures and new AI-driven diagnoses. To tap into these datasets, scientists explore techniques for using sensitive images without compromising identity. Most methods focus on face obfuscation (Newton, Sweeney, and Malin 2005), blurring (Frome et al. 2009), pixelation (Zhou and Pun 2020), warping (Korshunov and Ebrahimi 2013), affecting image saliency. Face-swapping (Hukkelås, Mester, and Lindseth 2019; Maximov, Elezi, and Leal-Taixé 2020; Chen et al. 2020; Gu et al. 2020;

*This work was primarily carried out during the internship of Zikui Cai at United Imaging Intelligence, Burlington, MA 01803. Copyright © 2024, Association for the Advancement of Artificial Intelligence (www.aaai.org). All rights reserved.

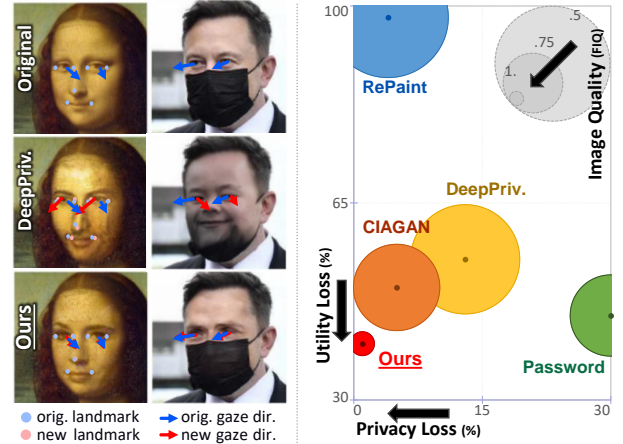


Figure 1: *Disguise* anonymizes face images while preserving their utility (i.e., attributes relevant to downstream tasks). For instance, facial landmarks and gaze direction are better preserved compared to existing methods, as shown in the figure that the red dots for landmarks and red arrows for gazes in the new images are more aligned with the blue ones in the original images. We outperform prior art by a large margin along various axes, including privacy, utility, and image quality. For image quality, small radius indicates higher FIQ (Terhorst et al. 2020) score and better image quality.

Cao et al. 2021; Proença 2021; Agarwal, Chattopadhyay, and Wang 2021) is emerging as a promising solution.

Popularized through the notion of *deepfakes* (Westerlund 2019), these deep-learning models are trained to replace any face in an image or video by another one (user-provided or AI-generated), while trying to preserve the overall saliency or specific facial attributes, such as perceived gender, expression, or hair color. While recent solutions can generate convincing results, they are not suitable for the targeted use cases as they lack formal *privacy* and *utility* guarantees for the resulting images. Face-swapping methods evade the confidentiality of the ID provider since the swapped face leaks the source ID. In addition, they lack proper mechanisms to maximize de-identification and minimize identity leakage of the target ID. Furthermore, they do not emphasize on maintaining the *utility* of resulting images, i.e., they do not guarantee that the altered images can have the same function

as the original ones for various downstream tasks. For example, a dataset would become *useless* for analysis if relevant non-biometric features are corrupted (e.g., facial expressions have changed for sentiment analysis tasks) or for training recognition models if the altered images no longer match their annotations (e.g., facial landmarks, gaze directions, head-pose orientations, etc.).

In this work, we aim to address the challenge of anonymizing images of individuals while ensuring privacy and maintaining high data utility. To this end, we propose *Disguise* (Deep Identity Swapper Guaranteeing Utility with Implicit Supervision from Experts), a de-identification method built upon face-swapping technology that offers formal guarantees regarding identity obfuscation and utility retention. Our main contributions are as follows:

- We propose a simple yet effective framework for face de-identification which generates natural faces with distinct identities from the original ones, while maintaining non-biometric attributes unchanged.
- Unlike existing methods that pre-discard original face IDs, we condition the synthetic faces on the original ID vectors and maximize the distance to the original identities while ensuring differential privacy (Dwork, Roth et al. 2014; Abadi et al. 2016), with randomization to prevent re-identification.
- We demonstrate superior results than state-of-the-art methods through extensive evaluation regarding the de-identification rate, utility preservation, and image quality of the resulting data over a large number of metrics.

Related work

Face Swapping. The topic of face swapping has received significant attention in research and is highly relevant, as evidenced by the large body of works dedicated to it (Nirkin, Keller, and Hassner 2019; Li et al. 2020; Perov et al. 2020; Chen et al. 2020; Zhu et al. 2021; Xu et al. 2022). However, it presents inherent and important differences compared to face anonymization/de-identification. Face swapping aims to change the original identity to a specified target identity, whereas face anonymization shall not rely on actual identities, as it would otherwise compromise both target and source individuals. Moreover, the two domains consider different performance indicators and evaluation metrics. Anonymization aims at providing privacy-preserving guarantees, including face anonymization rate and non-re-identifiability (Gross et al. 2005; Liu et al. 2021; Croft, Sack, and Shi 2021; Tölle et al. 2022), which implies additional mechanisms compared to the face-swapping methods that prioritize preserving facial attributes while reckoning the visual quality of the injected identity (Nirkin, Keller, and Hassner 2019; Xu et al. 2022).

Face Anonymization. Although traditional methods such as blacking out, pixelation, and Gaussian blur (Boyle, Edwards, and Greenberg 2000; Gross et al. 2006, 2009; Neustaedter, Greenberg, and Boyle 2006; Newton, Sweeney, and Malin 2005) are effective in removing privacy-sensitive information, they drastically alter the original data distribution, resulting in a significant loss in *utility*. In other

words, these methods generate anonymized images that are not suitable for downstream tasks such as gaze estimation (Kellnhofer et al. 2019; Zhang et al. 2020), head-pose prediction (Zhou and Gregson 2020; Hempel, Abdelrahman, and Al-Hamadi 2022), facial-landmarks regression (Deng et al. 2020; King 2009), and expression estimation (Wen et al. 2021; Savchenko 2022) due to the lack of necessary visual information.

A significant amount of research on face anonymization approaches the problem as an image inpainting task, where the face region is first erased and then replaced with another. Early methods (Gross et al. 2005; Padilla-López, Chaaoui, and Flórez-Revuelta 2015) use a database of real faces to aggregate the new identity, while more recent methods (Hukkelås, Mester, and Lindseth 2019; Maximov, Elezi, and Leal-Taixé 2020; Liu et al. 2021) use generative models to synthesize fake identities based on the learned distribution. DeepPrivacy (Hukkelås, Mester, and Lindseth 2019) is one of the pioneering works in this field, which reconstructs the missing face by taking the masked face and facial landmarks as inputs. However, the reconstructed face distribution suffers from bias as it is solely conditioned on its training data, leading to a tendency to generate smiling, young-looking faces. CIAGAN (Maximov, Elezi, and Leal-Taixé 2020) is another work that uses facial masks and landmarks to generate new faces. However, it tends to generate faces with duplicated identities due to the length limitation of the one-hot vector. RePaint (Lugmayr et al. 2022), a recent method based on diffusion models, generates photo-realistic faces with large facial variances, but it fails to maintain the utility of the faces and is sensitive to input distributions.

Some methods (Gu et al. 2020; Cao et al. 2021; Proença 2021) have focused on making the anonymization process reversible, such as *Password* (Gu et al. 2020) and *RiD-DLE* (Li et al. 2023), which generate anonymized faces conditioned on a password that can be used to de-anonymize them. While such a feature can be desirable in some scenarios, it violates privacy regulations like GDPR (Voigt and Von dem Bussche 2017) that protects *pseudonymous* data (data that has been de-identified from the data’s subject but can be re-identified as needed by the use of additional information). In this work, we propose to anonymize faces in an irreversible manner. Other solutions (Li and Lin 2019; Chen et al. 2021; Li and Clifton 2021; Liu et al. 2021) incorporate notions of differential privacy (Duchi, Jordan, and Wainwright 2013; Dwork, Roth et al. 2014; Abadi et al. 2016) by adding adequately-calibrated random noise either at training or inference time, ensuring privacy levels linked to their parameter ϵ . Or directly optimize in the latent space of StyleGAN (Barattin et al. 2023). However, they often neglect utility preservation (e.g., they edit image background and utility attributes) and require complex post-processing, making them not readily applicable to anonymization tasks.

Methodology

In this section, we formalize our objectives, theoretically ground our work, and finally describe our proposed solution.

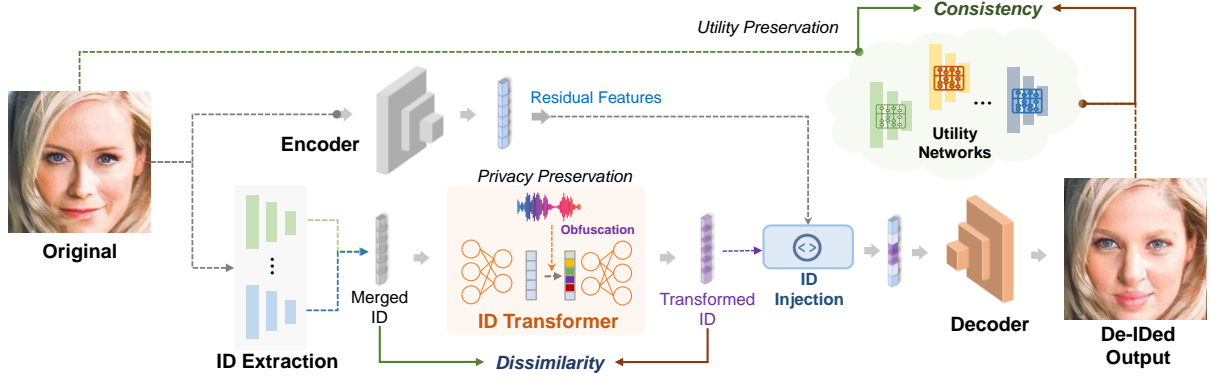


Figure 2: Illustration of the training process for the proposed *Disguise* framework. More discussions in Methodology Section.

Problem Formulation

Privacy Utility Dual Optimization. Let $\mathcal{X} \subset \mathbb{R}^{3 \times H \times W}$ be the image space, with $x \in \mathcal{X}$ an image depicting an individual. Let $(\mathcal{Z}, d_{\mathcal{Z}})$ be a metric space, with $\mathcal{Z} \subset \mathbb{R}^{n_{\mathcal{Z}}}$ space of identity-distilled facial features (*i.e.*, facial features that uniquely identify an individual) and $d_{\mathcal{Z}} : \mathcal{Z} \times \mathcal{Z} \rightarrow \mathbb{R}$ a distance function attached to space \mathcal{Z} . Let $(\mathcal{Y}, d_{\mathcal{Y}})$ be another metric space, with $\mathcal{Y} \subset \mathbb{R}^{n_{\mathcal{Y}}}$ containing utility-distilled facial features (*i.e.*, features that are useful to downstream tasks) and $d_{\mathcal{Y}} : \mathcal{Y} \times \mathcal{Y} \rightarrow \mathbb{R}$ a distance function relating to \mathcal{Y} . We note $f_{\mathcal{Z}} : \mathcal{X} \rightarrow \mathcal{Z}$ and $f_{\mathcal{Y}} : \mathcal{X} \rightarrow \mathcal{Y}$ the objective labeling functions respective to each domain.

We define a conditional generative function $G : \mathcal{X} \rightarrow \mathcal{X}$ parameterized by θ , that takes $x \in \mathcal{X}$ as input and returns an edited version $G(x) = \tilde{x}$. Our goal is to learn a G such that *utility* is maximized (*i.e.*, $f_{\mathcal{Y}}(x) = f_{\mathcal{Y}}(\tilde{x})$) and *privacy* is maximized (*i.e.*, $f_{\mathcal{Z}}(x)$ is distant from $f_{\mathcal{Z}}(\tilde{x})$). In other terms, the output of G should contain the same utility attributes as the input and contain identity attributes different from the input beyond recognition. Formally, we want G to achieve Pareto optimality (Sener and Koltun 2018; Momma, Dong, and Liu 2022) w.r.t. the aforementioned multiple objectives (*i.e.*, identity obfuscation and utility preservation), accounting for their possible competition (depending on downstream tasks, utility and identity attributes may overlap), thus minimizing the following objective:

$$\min_{\theta} \left(-\mathbb{E}_{x \in \mathcal{X}} [d_{\mathcal{Z}}(f_{\mathcal{Z}}(x), f_{\mathcal{Z}} \circ G_{\theta}(x))] \right), \quad (1)$$

$$\mathbb{E}_{x \in \mathcal{X}} [d_{\mathcal{Y}}(f_{\mathcal{Y}}(x), f_{\mathcal{Y}} \circ G_{\theta}(x))]^{\top}$$

Before tackling the challenges of multi-objective optimization that such a task brings, one has to consider how to model the unknown objective distance and labeling functions $d_{\mathcal{Z}}, f_{\mathcal{Z}}$ and $d_{\mathcal{Y}}, f_{\mathcal{Y}}$ for the identity and utility space respectively. We argue that identity and utility are conceptually subjective, *i.e.*, different authoritative entities have different definitions and target features assigned to each concept. *e.g.*, given a picture of a person, each human or algorithmic agent will rely on different features (facial landmarks, eye color, *etc.*) and their own subjective judgment to certify the person’s identity, as there is no absolute objective function to perform the ill-posed mapping of a facial

picture to an identity. Similarly, the concept of *utility* is conditioned by a set of target tasks or the agents in charge of said tasks. *e.g.*, an image with the person’s face completely blurred could still be *used* by a person-detection algorithm, but would be *useless* for facial landmark regression.

Therefore, we propose to rely on predefined agents (*experts*) to provide the identity and utility definitions to guide the optimization of our model (Gross et al. 2005). We thus consider some parameterized models $h_{\mathcal{Z}}$ and $h_{\mathcal{Y}}$ pre-optimized to approximate their respective objective labeling functions $f_{\mathcal{Z}}$ and $f_{\mathcal{Y}}$. Note that we make no assumption on the architecture or training of each of these models (we demonstrate with various state-of-the-art identity extraction and recognition models). Without loss of generality and to account for individual bias, we define $H_{\mathcal{Z}} = \{h_{\mathcal{Z}}^i\}_{i=1}^{k_{\mathcal{Z}}}$ and $H_{\mathcal{Y}} = \{h_{\mathcal{Y}}^i\}_{i=1}^{k_{\mathcal{Y}}}$ as sets of $k_{\mathcal{Z}}$ and $k_{\mathcal{Y}}$ unique models which differ in terms of architecture and/or training regime, *c.f.* mixture-of-experts theory (Miller and Uyar 1996; Masoudnia and Ebrahimpour 2014; Dai et al. 2021). We demonstrate in this paper how these identification/utilization experts can be leveraged in an adversarial/collaborative framework to train g towards a satisfying optimum.

Identity Obfuscation Guarantees. To provide formal de-identification guarantees, we ground our work in the extensive theory on ϵ -differential privacy (ϵ -DP) and ϵ -local-differential privacy (ϵ -LDP, relevant when obfuscation should be performed without global knowledge) applied to identity-swapping functions (Duchi, Jordan, and Wainwright 2013; Dwork, Roth et al. 2014; Abadi et al. 2016; Yu et al. 2020; Liu et al. 2021; Croft, Sack, and Shi 2021; Tölle et al. 2022; Qiu et al. 2022). Let $\psi : \mathcal{Z} \rightarrow \mathcal{Z}$ be a function that performs ID obfuscation, *i.e.*, taking an identity vector z and returning a new one \tilde{z} that maximizes $d_{\mathcal{Z}}(z, \tilde{z})$. We consider that an approximate but randomized function $\psi^{\epsilon} : \mathcal{Z} \rightarrow \mathcal{Z}$ satisfies ϵ -LDP if, for any two adjacent inputs $z, z' \in \mathcal{Z}$ and for any subset of outputs $Z_s \subseteq \text{range}(\psi^{\epsilon})$, it holds that $\mathbb{P}(\psi^{\epsilon}(z) \in Z_s) \leq e^{\epsilon} \mathbb{P}(\psi^{\epsilon}(z') \in Z_s)$. Given $\Delta\psi = \sup_{z, z' \in \mathcal{Z}} \|\psi(z) - \psi(z')\|_1$ the sensitivity of ψ , Laplace noise is commonly leveraged to define an ϵ -DP version of the function: $\psi^{\epsilon}(z) \triangleq \psi(z) + (\text{Lap}(\Delta\psi/\epsilon))^{n_{\mathcal{Z}}}$ (Duchi, Jordan, and Wainwright 2013; Dwork, Roth et al. 2014; Abadi et al. 2016; Liu et al. 2021). We demonstrate

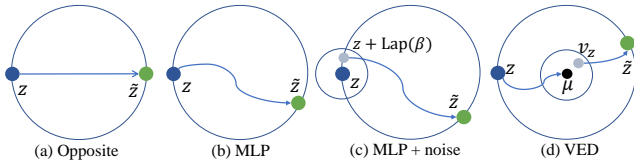


Figure 3: Identity transformation. The identity vector is normalized to the surface of a unit n-sphere.

that to ensure ϵ -LDP, the $d_{\mathcal{Z}}$ -maximization property of the identity-obfuscation function has to be relaxed. The manifold of identity vectors generated by an identification function $h_{\mathcal{Z}}$ is bounded by the range of said function. In such a space and for any Euclidean distance $d_{\mathcal{Z}}$, a non-relaxed version of ψ would be the bijective (and thus non-private) function ψ_{opp} mapping an ID vector to its opposite. No other function (e.g., ψ^{ϵ}) could ensure $d_{\mathcal{Z}}$ -maximization. Therefore, in this work, we consider the inherent trade-off between maximizing swapping-based identity obfuscation and ensuring differential privacy, and we propose a variety of solutions ψ^{ϵ} tailored to different needs (as illustrated in Figure 3, and more details in Proposed Solution Section).

Non Re-identifiability. Another important aspect to consider in privacy-preserving applications is *non-invertibility*. If the de-identified data can be re-identified with additional information, then the operation is not truly anonymization but *pseudonymization*. For example, with the correct password for Password (Gu et al. 2020) and RiDDLE (Li et al. 2023), or using the opposite ID for ψ_{opp} , the original ID is compromised. We empirically demonstrate that the proposed obfuscation solutions achieve varying degrees of robustness to such re-identification efforts.

In the remaining of the section, we explain how we define and train g to ensure privacy-preserving non-invertible identity swapping in images and utility preservation.

Proposed Solution

The proposed architecture can be defined as the composition of a face-swapping model $g : \mathcal{X} \times \mathcal{Z} \rightarrow \mathcal{X}$, an identity extractor $h_{\mathcal{Z}} : \mathcal{X} \rightarrow \mathcal{Z}$, and an identity obfuscation function $\psi^{\epsilon} : \mathcal{Z} \rightarrow \mathcal{Z}$, such that $G(x) = g(x, \psi^{\epsilon} \circ h_{\mathcal{Z}}(x))$. Given a facial image x , $h_{\mathcal{Z}}$ extracts the vector z encoding the identity of the depicted person. This vector z is passed to the privacy-enabling function ψ^{ϵ} , which returns a synthetic identity \tilde{z} that maximizes obfuscation. Finally, the face-swapper model g edits the original image x to inject the fake identity \tilde{z} , resulting in an image \tilde{x} where the original visual identifying attributes are replaced by those encoded in \tilde{z} . Additionally, during its training, g relies on the feedback of tasks-specific models $h_{\mathcal{Y}}^i : \mathcal{X} \rightarrow \mathcal{Y}$ to ensure that the utility of \tilde{x} is maintained compared to x . We expand on each block in the following paragraphs.

Identity Extraction. As mentioned in Section , we propose to extract the identity information from facial images via model ensembling (Miller and Uyar 1996; Masoudnia and Ebrahimpour 2014; Dai et al. 2021), to ensure generalizability as well as to limit the impact of models’ bias (as we assume no control over the architecture or training reg-

imen of selected identity-expert models). Therefore, given a set $H_{\mathcal{Z}} = \{h_{\mathcal{Z}}^i\}_{i=1}^{k_{\mathcal{Z}}}$ of ID extractors, we define $h_{\mathcal{Z}}$ as the ensemble method $h_{\mathcal{Z}}(x) = \text{MLP}_{\theta_z}(\parallel_{i=1}^{k_{\mathcal{Z}}} h_{\mathcal{Z}}^i(x))$, i.e., concatenating (symbol \parallel) the $k_{\mathcal{Z}}$ predicted vectors together and merging them into $z \in \mathcal{Z}$ via a multilayer perceptron (MLP) with parameters θ_z and tanh as final activation.

Identity Transformation. A variety of techniques can be considered to perform the identity transformation ψ , as shown in Figure 3. If we were to maximize the distance between the original and obfuscating IDs, the optimal function would be $\psi_{\text{opp}}(z) = -z$ since $\arg \max_{z'} d_{\mathcal{Z}}(z, z') = -z$ in our normalized Euclidean identity space. However, such a function is reversible, making it easy to re-identify the original individual by taking the opposite of the pseudonymized ID. A more secure solution would be a parametric function, e.g., $\psi_{\text{mlp}}(z) = \text{MLP}_{\theta_{\psi}}(z)$, trained to optimally fool $h_{\mathcal{Z}}$. As a non-explicit function, ψ_{mlp} is more challenging to invert, though not impossible with the access to the model or its parameters θ_{ψ} (c.f. gradient-based attacks (Fredrikson, Jha, and Ristenpart 2015; Wang, Si, and Wu 2015)). To increase robustness and ensure ϵ -LDP, we can add dimension-wise noise to the inner operation, i.e., $\psi_{\text{mlp}}^{\epsilon}(z) = \text{MLP}_{\theta_{\psi}}(z + (\text{Lap}(\beta))^{n_z})$, with $\beta = \frac{\Delta \psi_{\text{mlp}}}{\epsilon}$. The larger β is set (i.e., the smaller ϵ is), the more noise is applied to the original ID vector before further MLP-based obfuscation. Therefore, larger β provides stricter privacy guarantee and robustness but adversarial affects the ability of $\psi_{\text{mlp}}^{\epsilon}$ to learn how to fool identification experts $H_{\mathcal{Z}}$.

To better navigate this trade-off and guarantee a more continuous space for the noise application, we leverage the properties inherent to variational autoencoders (VAEs) (Kingma and Welling 2013). We introduce a variational encoder-decoder (VED) to transform the identity vector, i.e., $\psi_{\text{ved}}^{\epsilon}(z) = \text{VED}_{\theta_{\psi}}(z)$. This model’s encoder predicts the parameters (μ, σ) of the latent data distribution (assumed to be Gaussian). A latent vector v_z is picked as $\mu + \sigma \eta$ with $\eta \sim (\mathcal{N}(0, 1))^{n_v}$ (c.f. reparameterization (Kingma, Salimans, and Welling 2015)) then passed to the decoder. While a VAE decoder would reconstruct the input identity from v_z , our VED decoder should generate a new, distant identity. During inference, we sample v_z as $\mu + \sigma (\text{Lap}(\alpha))^{n_v}$ to meet ϵ -LDP, with n_v dimension of latent space and $\alpha = \frac{\Delta \psi_{\text{ved}}}{\epsilon}$. To train either of these models, we enforce cosine dissimilarity between the original and generated ID vectors:

$$\mathcal{L}_{\text{deid}} = 1 + \frac{z \cdot \tilde{z}}{\|z\|_2 \|\tilde{z}\|_2}. \quad (2)$$

For the VED model, we add to this criterion the usual Kullback–Leibler divergence (KLD) loss \mathcal{L}_{kld} (Kingma, Salimans, and Welling 2015; Kingma and Welling 2013).

Face Swapping. Once the fake identity vector \tilde{z} is generated, it is passed to the face-swapping model g , along with the original image x . Similar to existing solutions (Chen et al. 2020; Perov et al. 2020; Liu et al. 2021), g is composed of three modules: (1) an image encoder that extracts identity-unrelated features ν ; (2) an ID injector that aggregates ν and \tilde{z} into a vector encoding the content of the obfus-

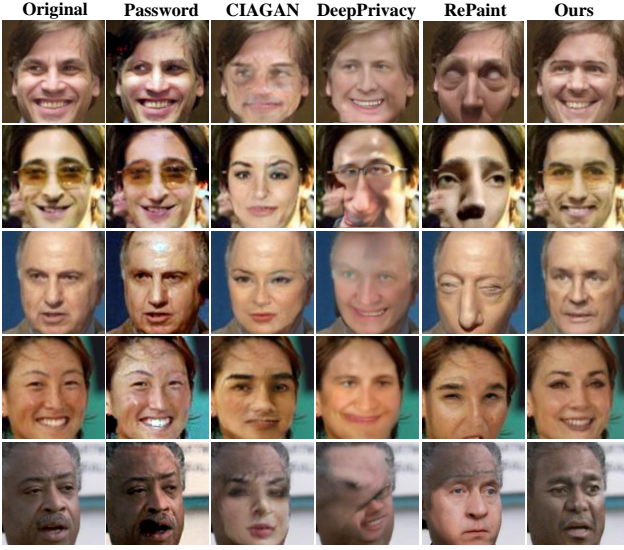


Figure 4: Qualitative results of different methods. Ours preserves utility while anonymizing identities.

cated image \tilde{x} ; (3) a decoder conditioned on this vector that generates \tilde{x} . These existing works also share similar losses that we borrow and adapt:

$$\begin{aligned}\mathcal{L}_{\text{mix}} &= \|g(x, \tilde{z}) - g(x, z)\|_1; \\ \mathcal{L}_{\text{gen}} &= \sum_{i=1}^{k_d} \log(1 - D_i(x, \tilde{x})); \\ \mathcal{L}_{\text{id}} &= \sum_{\hat{z} \in \{z, \tilde{z}\}} \left(1 - \frac{\hat{z} \cdot \hat{z}_h}{\|\hat{z}\|_2 \|\hat{z}_h\|_2}\right);\end{aligned}\quad (3)$$

with $\hat{z}_h = h_{\mathcal{Z}}(g(x, \hat{z}))$. Here, \mathcal{L}_{mix} is a mixing loss to ensure implicit disentanglement of ID features (encoded in z or \tilde{z}) and residual features (*i.e.*, ν). \mathcal{L}_{gen} pits the generator against k_d discriminators D to ensure realistic results preserving image saliency, *c.f.* recent GAN solutions (Wang et al. 2018; Hukkelås, Mester, and Lindseth 2019; Chen et al. 2020) (we also use their weak-feature matching loss, further ensuring the high-level semantic alignment between the image pairs). Finally, \mathcal{L}_{id} enforces cosine similarity between the injected identity \hat{z} and the one observed by the identification model $h_{\mathcal{Z}}$ in the resulting image. Combined together, along with $\mathcal{L}_{\text{deid}}$ and \mathcal{L}_{kld} (using weighting hyperparameters), these losses form the overall objective for our privacy-enforcing face-swapping solution G .

Utility Preservation. Existing face-swapping methods (Hukkelås, Mester, and Lindseth 2019; Chen et al. 2020; Perov et al. 2020; Liu et al. 2021) claim that their adversarial and feature-matching losses ensure the preservation of non-identifying content. However, such supervision is too weak to guarantee that the images will maintain their utility w.r.t. downstream tasks, especially for tasks relying on small attention regions (*e.g.*, gaze estimation). We thus complement the aforementioned objective with a criterion that leverages the implicit expertise of tasks-relevant models $H_{\mathcal{Y}}$:

$$\mathcal{L}_{\text{uti}} = \sum_{i=1}^{k_{\mathcal{Y}}} \lambda_{\text{uti},i} \|h_{\mathcal{Y}}^{i,l}(x) - h_{\mathcal{Y}}^{i,l}(\tilde{x})\|_1, \quad (4)$$

with $h_{\mathcal{Y}}^{i,l}(\cdot)$ the features returned by the last differential non-softmax layer l of model $h_{\mathcal{Y}}^i$, and $\lambda_{\text{uti}} \in \mathbb{R}^{k_{\mathcal{Y}}}$ hyperparameters weighting the task/expert contributions. Hence, \mathcal{L}_{uti} imposes that altered images contains the same utility attributes as original images, as expected by tasks-relevant models.

Note that the entire solution $G(x) = g(x, \psi^e \circ h_{\mathcal{Z}}(x))$ is end-to-end differentiable, thus single-pass trainable. In practice, we leverage its modularity and train each component separately before jointly fine-tuning. Scalar hyperparameters weigh the contribution of each loss to the total objective (we fix $\{\lambda_{\text{id}}, \lambda_{\text{deid}}, \lambda_{\text{mix}}, \lambda_{\text{uti,eye}}, \lambda_{\text{uti,emo}}, \lambda_{\text{kld}}\} = \{30, 30, 10, 2, 2, 0.2\}$).

Experiments

We now describe our experimental setup and compare with other methods in terms of privacy robustness and data usability. More details in supplementary material.

Experimental Protocol

Datasets. We use multiple datasets for training and evaluation. We train our models on VGGFace2 dataset (Cao et al. 2018), which totals 3.31 million images with 9,131 identities. We use multiple datasets for evaluation, including LFW (Huang et al. 2008) (13,233 face images and 5,749 identities) for utility and de-identification performance, CelebA-HQ (Karras et al. 2017) (30,000 face images) for utility evaluation, and WFLW (Wu et al. 2018) (10,000 face images) for the training usability w.r.t. the downstream task of landmark detection.

Identity and Utility Models. To demonstrate the genericity of our method, we consider a variety of pretrained face-identification networks and of utility networks over different recognition tasks. As identity experts, we use ArcFace (Deng et al. 2019), AdaFace (Kim, Jain, and Liu 2022), FaceNet (Schroff, Kalenichenko, and Philbin 2015), and SphereFace (Liu et al. 2017). Either ArcFace ($h_{\mathcal{Z}}^{\text{arc}}$), AdaFace ($h_{\mathcal{Z}}^{\text{ada}}$), or both ($h_{\mathcal{Z}}^{\text{mix}}$) are used to guide g during training (*c.f.* Equation 4); FaceNet and SphereFace are used only for evaluation. For the downstream tasks, we use ETH-XGaze (Zhang et al. 2020) (noted $h_{\mathcal{Y}}^{\text{eye}}$) for gaze estimation, DAN (Wen et al. 2021) ($h_{\mathcal{Y}}^{\text{emo}}$) for facial expression recognition, or both ($h_{\mathcal{Y}}^{\text{mix}}$) to provide utility feedback during training. During evaluation, we use L2CS-Net (Abdelrahman et al. 2022) for gaze estimation, DeepFace (DF) (Serengil and Ozpinar 2021) for emotion recognition, and RetinaFace (Deng et al. 2020) and Dlib (King 2009) for landmark detection.

Metrics. We employ the commonly-used validation rate and verification accuracy as metrics for evaluating privacy preservability (Schroff, Kalenichenko, and Philbin 2015; Liu et al. 2017; Deng et al. 2019; Kim, Jain, and Liu 2022). The validation rate is defined as the true positive rate (TPR) at certain false positive rate (FPR), *e.g.*, TPR @ FPR=1e-3. Verification accuracy is the percentage of image pairs correctly classified as the same/different person using the best

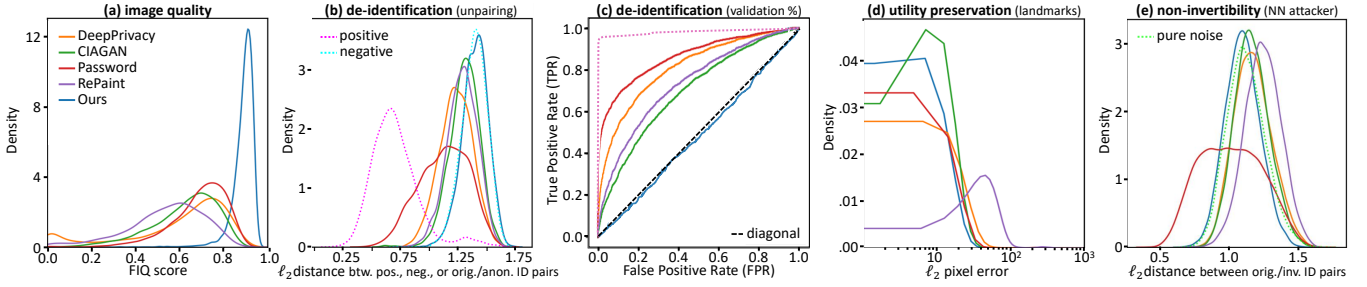


Figure 5: *Disguise* outperforms existing methods in various aspects, including image quality, de-id rate, and utility. For non-invertibility, our solution is close to other methods that completely erase the original IDs (*i.e.*, recovering pure Gaussian noise).

ℓ_2 distance threshold. The verification accuracy of random guessing is thus 50%, which is what anonymization aims at. To measure utility preservation, we use ℓ_2 pixel distance and normalized mean error (NME) for facial landmark detection, mean absolute error (MAE) for gaze estimation, and accuracy for emotion recognition. For image quality, we use SER-FIQ (Terhorst et al. 2020).

Comparison. We consider various de-identification methods, including DeepPrivacy (Hukkelås, Mester, and Lindseth 2019), DeepPrivacy2 (Hukkelås and Lindseth 2023), CIA-GAN (Maximov, Elezi, and Leal-Taixé 2020), Password (Gu et al. 2020), and RePaint (Lugmayr et al. 2022). For readability of the tables, we denote different versions as “Ours (*a*, *b*, *c*)” where *a* fixes the identity model(s) h_Z^a used, *b* the transformation function ψ_b^c , and *c* the utility model(s) h_Y^c . For simplicity, we use “Ours (arc, ved, eye)” as our default method unless otherwise mentioned. We demonstrate the impact of different transformation models and identity/utility experts in ablation studies.

Privacy: Obfuscation Evaluation

De-identification performance. As shown in Table 1, we achieve near perfect de-id rate, *i.e.*, with a validation rate close to 0 and verification accuracy close to 50%, outperforming other methods by a significant margin, and is even more secure than randomly picking replacement images from the dataset. Figure 5(b) presents the ℓ_2 distance histogram for original positive pairs, original negative pairs, and original-anonymized positive pairs on LFW (Huang et al. 2008), and Figure 5(c) shows the ROC curves of validation rate. We observe that *Disguise* creates image pairs that are close to the negative distribution, hence perfect obfuscation. We also achieve the highest facial image quality, see Figures 1 and 4 for visual reference. Among other comparing methods, it is worth noticing that Password fails to de-identify images, hence the highest validation rate. CIA-GAN and RePaint are better than Password in de-identification, however they suffer from low facial image quality due to high artifacts and distortions.

Original and anonymized ID de-correlation. We consider scenarios where malicious attackers attempt to link anonymized IDs with their original IDs, allowing them to perform inversion inference on the anonymized IDs and recover the original ones. We use encoder-decoder networks to learn the correlation on existing original-anonymized image pairs. Figure 5(e) shows the results of using MLPs to decode

Table 1: Identification / validation rate and image quality evaluation over edited LFW data.

Methods	TPR (%) @ FPR= 10^{-3} / Accuracy (%) ↓		Accuracy (%) ↓		FIQ ↑ SER
	FaceNet	SphereFace	AdaFace	Average	
Original	93.8 / 97.1	87.9 / 96.2	95.4 / 97.7	92.4 / 97.0	0.77
DeepPrivacy	7.3 / 73.8	2.9 / 70.9	4.6 / 68.6	4.9 / 71.1	0.67
DeepPrivacy2	1.7 / 62.5	1.0 / 61.5	2.2 / 62.2	1.6 / 62.1	0.68
CIA-GAN	1.8 / 64.5	1.0 / 59.0	5.6 / 71.0	2.8 / 64.8	0.58
Password	31.7 / 79.1	17.1 / 73.5	51.0 / 84.0	33.3 / 78.9	0.69
RePaint	2.8 / 67.7	1.1 / 63.5	3.6 / 68.5	2.5 / 66.6	0.54
Ours	0.03 / 50.0	0.03 / 50.0	0.00 / 50.0	0.02 / 50.0	0.90

obfuscated IDs from CelebA-HQ (Karras et al. 2017) while trained on LFW (Huang et al. 2008) using original IDs as supervision. While methods like DeepPrivacy, CIA-GAN, and RePaint are inherently robust to inversion attacks since the original face region is entirely erased, and their networks are solely tasked with inpainting the blank region, our method still offers de-correlation on par with these methods, suggesting that our method is also resilient to inversion attacks.

Utility: Usability Evaluation

Utility corruption in anonymized images. Our method demonstrates superior utility preservation compared to others across datasets (Table 2). We highlight our approach’s excellence through qualitative comparison (Figure 1 and 4). DeepPrivacy lacks facial attribute preservation, exhibiting bias towards smiles and youth. CIA-GAN bears heavy artifacts; Password yields blurry and easily re-identifiable outcomes. RePaint excels with in-distribution faces (RePaint is trained on CelebA-HQ thus has improved performance on the same dataset in Table 2), but it fails elsewhere and doesn’t retain original attributes. For challenging scenarios, like heavy occlusion (*e.g.*, masks), CIA-GAN and DeepPrivacy falter, unlike our effective face-swapping model.

Usability of anonymized images as training data. We have demonstrated utility attribute non-corruption by comparing performance of pretrained task-specific models on obfuscated versus original data. Now, we advance toward the initial motivation of data anonymization for new solutions, evaluating how utility networks trained from scratch on anonymized data perform on real, unseen samples. Ideally, these privacy-preprocessed models should match performance of those trained on original, non-obfuscated data. Taking facial landmark detection as an example on the WFLW dataset (Wu et al. 2018) (98 landmarks per image), we split data into training/testing sets (7,500/2,500) and

Table 2: Utility performance comparison of different anonymization methods over diverse downstream tasks on LFW and CelebA-HQ datasets (Huang et al. 2008; Karras et al. 2017).

Dataset	Methods	Facial landmarks (L2 pixel distance ↓)								Gaze estimation (MAE° ↓)				Emotion	
		RetinaFace (5 points)				Dlib (68 points)				L2CS-Net		ETH-XGaze		(Accuracy % ↑)	
		All	Eyes	Nose	Mouth	All	Eyes	Nose	Mouth	Pitch	Yaw	Pitch	Yaw	DAN	DF
LFW	DeepPrivacy	23.9	13.1	9.9	16.5	263.0	32.7	25.1	89.0	7.7	13.6	8.0	16.3	27.1	34.3
	DeepPrivacy2	31.2	18.4	14.4	19.6	385.7	59.9	49.9	120.6	9.2	12.2	7.8	15.1	22.4	30.2
	CIAGAN	14.6	9.3	5.5	9.2	348.2	59.0	31.2	97.7	8.8	14.6	7.8	16.9	32.5	36.9
	Password	17.4	10.4	7.7	11.1	204.8	26.5	19.3	55.4	10.5	24.7	7.7	11.5	45.9	43.4
	RePaint	66.1	30.8	32.2	47.3	1103.1	133.5	152.1	432.0	11.3	18.1	9.2	18.8	17.3	19.4
	Ours	12.9	7.7	5.6	8.2	203.3	28.8	19.8	60.0	6.8	8.4	5.6	10.0	46.2	47.0
CelebA-HQ	DeepPrivacy	13.1	4.8	4.3	10.8	293.9	30.4	24.2	113.0	7.0	8.7	6.7	10.1	41.0	45.5
	CIAGAN	14.9	10.3	4.6	8.6	365.6	79.2	35.6	91.5	8.7	13.7	7.5	13.4	38.0	44.4
	RePaint	9.9	3.0	4.6	7.5	249.1	22.7	29.7	95.9	6.2	8.0	5.5	8.0	50.4	55.8
	Ours	6.7	3.4	3.3	4.3	196.0	25.1	20.0	59.9	5.6	6.2	4.6	5.9	61.9	59.6

Table 3: Usability of de-identified datasets for the training of task-specific models (facial landmark detection on WFLW).

Methods	all	Normalized Mean Error (NME) ↓					
		pose	illu	occ	blur	mu	exp
Original	.039	.068	.039	.047	.045	.038	.043
DeepPrivacy	.058	.100	.057	.072	.066	.060	.066
CIAGAN	.055	.087	.054	.064	.061	.053	.060
Ours	.047	.079	.047	.056	.054	.046	.050

Table 4: Re-identifiability of our ID transformation methods.

Methods	TPR (%) @ FPR=1e-3 ↓ (LFW data)			
	Swapped		Inverted	
	FaceNet	Sph.Face	FaceNet	Sph.Face
Ours (arc, opp, \emptyset)	0.63	0.03	67.03	53.07
Ours (arc, ved, emo)	0.23	0.00	12.03	7.10
Ours (arc, ved, eye)	0.03	0.03	13.03	6.43
Ours (arc, mlp, eye)	0.00	0.00	52.90	45.97
Ours (arc, mlp, emo)	0.03	0.00	49.77	45.97
Ours (arc, mlp, <u>mix</u>)	0.00	0.00	50.23	44.67
Ours (<u>mix</u> , mlp, eye)	0.07	0.00	36.70	34.70

generate obfuscated training data using mentioned methods (test data remains unaltered). We use an HRNetv2-W18 model (Wang et al. 2021) for the task, trained for 60 epochs with Adam optimizer (Kingma and Ba 2014) ($\beta_1 = 0$, $\beta_2 = 0.999$), learning rate 10^{-4} , and batch size 64. Table 3 shows models on obfuscated data perform worse (higher NME of facial landmarks) than the one on original data. Our anonymized data model demonstrates the smallest accuracy drop, confirming higher utility preservation for downstream tasks while maintaining privacy.

Ablation Study

Here we demonstrate the impact of different transformation models, identity and utility experts.

Impact of transformation models on re-identifiability. As justified in Section and experimentally measured in Table 4, ψ_{opp} would suffer high re-identification, *i.e.* we can recover the original ID using the opposite of transformed ID. MLP-based transformations outperforms opposite transformation but VED-based transformations yield the best results in terms of de-identification and non-invertibility, confirming the superiority of our proposed solution.

The introduction of stochastic operations in alignment

Table 5: Effect of ψ^ϵ noise w.r.t. (re-)identifiability.

Methods		TPR (%) @ FPR=1e-3 ↓ (LFW data)			
Network	Noise	Swapped		Inverted	
		FaceNet	Sph.Face	FaceNet	Sph.Face
MLP	$\beta = 0.0$	0.00	0.00	52.90	45.97
	$\beta = 0.5$	0.40	0.00	23.20	20.80
	$\beta = 0.9$	5.90	2.50	3.07	1.30
	$\alpha = 1.0$	0.03	0.03	13.03	6.43
VED	$\alpha = 2.0$	0.37	0.00	7.43	3.20
	$\alpha = 3.0$	0.37	0.10	5.37	2.23

with ϵ -LDP further strengthen the solution. As shown in Table 5, the higher the amount of β or α noise introduced (*i.e.*, the lower ϵ), the more robust to attacks the method becomes, but the lower the original de-identification rate (the noisier the data, the harder it is to synthesize an ID that maximizes obfuscation). This negative impact is however better mitigated by the proposed VED. We provide further insights in supplementary material.

Effects of using multiple ID extractors. As shown in Table 4, MLP-based transformations relying on multiple identity extractors, *i.e.*, “Ours (mix, mlp, eye)”, perform better than versions with only one ID expert. We attribute the increased robustness to the combined knowledge of the two algorithms which capture more varied ID-related features that are then obfuscated.

Conclusion and Discussion

We introduced *Disguise*, a privacy-enhancing face de-identification model that ensures both depicted people’s privacy and image usability. Our experiments demonstrate its effectiveness in pre-processing sensitive data for inference or training. Rooted in privacy and mixture-of-experts theory, it outperforms prior methods in re-identification robustness and utility preservation.

Limitations. Note that our model is tailored for face obfuscation and does not address other identity-revealing visual attributes (*e.g.*, distinctive glasses, haircuts, backgrounds). Broader ID-extracting methods like H_Z (Bhanu, Kumar et al. 2017) could potentially handle this. Additionally, *Disguise* might benefit from multi-objective learning research (Désidéri 2012; Momma, Dong, and Liu 2022) to optimize cases where identity and utility features overlap.

Acknowledgments

Z. Cai and M. Asif were supported in part by AFOSR award FA9550-21-1-0330 and ONR award N00014-19-1-2264.

References

2003. Health Insurance Portability and Accountability Act. U.S. Department of Health and Human Services. 45 CFR Parts 160, 162, and 164.
2018. California Consumer Privacy Act. California Legislative Information. Cal. Civ. Code §1798.100 et seq.
2021. Personal Information Protection Law. National People's Congress of the People's Republic of China.
2022. InsightFace: 2D and 3D Face Analysis Project. <https://github.com/deepinsight/insightface>.
- Abadi, M.; Chu, A.; Goodfellow, I.; McMahan, H. B.; Mironov, I.; Talwar, K.; and Zhang, L. 2016. Deep learning with differential privacy. In *ACM CCS*.
- Abdelrahman, A. A.; Hempel, T.; Khalifa, A.; and Al-Hamadi, A. 2022. L2CS-Net: Fine-Grained Gaze Estimation in Unconstrained Environments. *arXiv:2203.03339*.
- Agarwal, A.; Chattopadhyay, P.; and Wang, L. 2021. Privacy preservation through facial de-identification with simultaneous emotion preservation. *SIVP*, 15(5).
- Barattin, S.; Tzelepis, C.; Patras, I.; and Sebe, N. 2023. Attribute-preserving Face Dataset Anonymization via Latent Code Optimization. In *CVPR*.
- Bhanu, B.; Kumar, A.; et al. 2017. *Deep learning for biometrics*, volume 7. Springer.
- Boyle, M.; Edwards, C.; and Greenberg, S. 2000. The effects of filtered video on awareness and privacy. In *CSCW*.
- Cao, J.; Liu, B.; Wen, Y.; Xie, R.; and Song, L. 2021. Personalized and Invertible Face De-identification by Disentangled Identity Information Manipulation. In *ICCV*.
- Cao, Q.; Shen, L.; Xie, W.; Parkhi, O. M.; and Zisserman, A. 2018. VGGFace2: A dataset for recognising faces across pose and age. In *International Conference on Automatic Face and Gesture Recognition*.
- Chen, J.-W.; Chen, L.-J.; Yu, C.-M.; and Lu, C.-S. 2021. Perceptual Indistinguishability-Net (PI-Net): Facial image obfuscation with manipulable semantics. In *CVPR*.
- Chen, R.; Chen, X.; Ni, B.; and Ge, Y. 2020. Simswap: An efficient framework for high fidelity face swapping. In *ACM International Conference on Multimedia*.
- Croft, W. L.; Sack, J.-R.; and Shi, W. 2021. Obfuscation of images via differential privacy: From facial images to general images. *P2PNA*, 14(3).
- Dai, Y.; Li, X.; Liu, J.; Tong, Z.; and Duan, L.-Y. 2021. Generalizable person re-identification with relevance-aware mixture of experts. In *CVPR*.
- Deng, J.; Guo, J.; Ververas, E.; Kotsia, I.; and Zafeiriou, S. 2020. Retinaface: Single-shot multi-level face localisation in the wild. In *CVPR*.
- Deng, J.; Guo, J.; Xue, N.; and Zafeiriou, S. 2019. ArcFace: Additive Angular Margin Loss for Deep Face Recognition. In *CVPR*.
- Désidéri, J.-A. 2012. Multiple-gradient descent algorithm (MGDA) for multiobjective optimization. *Comptes Rendus Mathématique*, 350(5-6).
- Duchi, J. C.; Jordan, M. I.; and Wainwright, M. J. 2013. Local privacy and statistical minimax rates. In *FOCS*. IEEE.
- Dwork, C.; Roth, A.; et al. 2014. The algorithmic foundations of differential privacy. *Foundations and Trends in Theoretical Computer Science*, 9(3-4).
- Fredrikson, M.; Jha, S.; and Ristenpart, T. 2015. Model inversion attacks that exploit confidence information and basic countermeasures. In *ACM CCS*.
- Frome, A.; Cheung, G.; Abdulkader, A.; Zennaro, M.; Wu, B.; Bissacco, A.; Adam, H.; Neven, H.; and Vincent, L. 2009. Large-scale privacy protection in google street view. In *ICCV*.
- Gross, R.; Airoldi, E.; Malin, B.; and Sweeney, L. 2005. Integrating utility into face de-identification. In *International Workshop on Privacy Enhancing Technologies*. Springer.
- Gross, R.; Sweeney, L.; Cohn, J.; Torre, F. d. l.; and Baker, S. 2009. Face de-identification. In *Protecting privacy in video surveillance*. Springer.
- Gross, R.; Sweeney, L.; De la Torre, F.; and Baker, S. 2006. Model-based face de-identification. In *CVPR workshop*.
- Gu, X.; Luo, W.; Ryoo, M. S.; and Lee, Y. J. 2020. Password-conditioned anonymization and deanonymization with face identity transformers. In *ECCV*. Springer.
- Hempel, T.; Abdelrahman, A. A.; and Al-Hamadi, A. 2022. 6D Rotation Representation For Unconstrained Head Pose Estimation. *arXiv:2202.12555*.
- Huang, G. B.; Mattar, M.; Berg, T.; and Learned-Miller, E. 2008. Labeled faces in the wild: A database for studying face recognition in unconstrained environments. In *Workshop on faces in 'Real-Life' Images*.
- Hukkelås, H.; and Lindseth, F. 2023. Deepprivacy2: Towards realistic full-body anonymization. In *WACV*.
- Hukkelås, H.; Mester, R.; and Lindseth, F. 2019. Deepprivacy: A generative adversarial network for face anonymization. In *ISVC*. Springer.
- Karras, T.; Aila, T.; Laine, S.; and Lehtinen, J. 2017. Progressive growing of gans for improved quality, stability, and variation. *arXiv:1710.10196*.
- Kellnhofer, P.; Recasens, A.; Stent, S.; Matusik, W.; and Torralba, A. 2019. Gaze360: Physically unconstrained gaze estimation in the wild. In *ICCV*.
- Kim, M.; Jain, A. K.; and Liu, X. 2022. AdaFace: Quality Adaptive Margin for Face Recognition. In *CVPR*.
- King, D. E. 2009. Dlib-ml: A Machine Learning Toolkit. *Journal of Machine Learning Research*, 10.
- Kingma, D. P.; and Ba, J. 2014. Adam: A method for stochastic optimization. *arXiv:1412.6980*.
- Kingma, D. P.; Salimans, T.; and Welling, M. 2015. Variational dropout and the local reparameterization trick. *NeurIPS*, 28.
- Kingma, D. P.; and Welling, M. 2013. Auto-encoding variational bayes. *arXiv:1312.6114*.

- Korshunov, P.; and Ebrahimi, T. 2013. Using warping for privacy protection in video surveillance. In *DSP*, 1–6. IEEE.
- Li, D.; Wang, W.; Zhao, K.; Dong, J.; and Tan, T. 2023. RiD-DLE: Reversible and Diversified De-identification with Latent Encryptor. In *CVPR*.
- Li, L.; Bao, J.; Yang, H.; Chen, D.; and Wen, F. 2020. Faceshifter: Towards high fidelity and occlusion aware face swapping. In *CVPR*.
- Li, T.; and Clifton, C. 2021. Differentially private imaging via latent space manipulation. In *SP*.
- Li, T.; and Lin, L. 2019. Anonymousnet: Natural face de-identification with measurable privacy. In *CVPR workshop*.
- Liu, B.; Ding, M.; Xue, H.; Zhu, T.; Ye, D.; Song, L.; and Zhou, W. 2021. Dp-image: differential privacy for image data in feature space. *arXiv:2103.07073*.
- Liu, W.; Wen, Y.; Yu, Z.; Li, M.; Raj, B.; and Song, L. 2017. SphereFace: Deep Hypersphere Embedding for Face Recognition. In *CVPR*.
- Lugmayr, A.; Danelljan, M.; Romero, A.; Yu, F.; Timofte, R.; and Van Gool, L. 2022. Repaint: Inpainting using denoising diffusion probabilistic models. In *CVPR*.
- Masoudnia, S.; and Ebrahimpour, R. 2014. Mixture of experts: a literature survey. *ARTR*, 42(2).
- Maximov, M.; Elezi, I.; and Leal-Taixé, L. 2020. Ciagan: Conditional identity anonymization generative adversarial networks. In *CVPR*.
- Miller, D. J.; and Uyar, H. 1996. A mixture of experts classifier with learning based on both labelled and unlabelled data. *NeurIPS*, 9.
- Momma, M.; Dong, C.; and Liu, J. 2022. A multi-objective/multi-task learning framework induced by Pareto stationarity. In *ICML*. PMLR.
- Neustaedter, C.; Greenberg, S.; and Boyle, M. 2006. Blur filtration fails to preserve privacy for home-based video conferencing. *TOCHI*, 13(1).
- Newton, E. M.; Sweeney, L.; and Malin, B. 2005. Preserving privacy by de-identifying face images. *TKDE*, 17(2).
- Nirkin, Y.; Keller, Y.; and Hassner, T. 2019. Fsgan: Subject agnostic face swapping and reenactment. In *ICCV*.
- Padilla-López, J. R.; Chaaraoui, A. A.; and Flórez-Revuelta, F. 2015. Visual privacy protection methods: A survey. *Expert Systems with Applications*, 42(9).
- Perov, I.; Gao, D.; Chervoniy, N.; Liu, K.; Marangonda, S.; Umé, C.; Dpfks, M.; Facenheim, C. S.; RP, L.; Jiang, J.; et al. 2020. DeepFaceLab: Integrated, flexible and extensible face-swapping framework. *arXiv:2005.05535*.
- Proença, H. 2021. The uu-net: Reversible face de-identification for visual surveillance video footage. *TCSVT*, 32(2).
- Qiu, Y.; Niu, Z.; Song, B.; Ma, T.; Al-Dhelaan, A.; and Al-Dhelaan, M. 2022. A Novel Generative Model for Face Privacy Protection in Video Surveillance with Utility Maintenance. *Applied Sciences*, 12(14): 6962.
- Savchenko, A. V. 2022. Video-Based Frame-Level Facial Analysis of Affective Behavior on Mobile Devices Using EfficientNets. In *CVPR*.
- Schroff, F.; Kalenichenko, D.; and Philbin, J. 2015. FaceNet: A unified embedding for face recognition and clustering. In *CVPR*.
- Sener, O.; and Koltun, V. 2018. Multi-task learning as multi-objective optimization. *NeurIPS*, 31.
- Serengil, S. I.; and Ozpinar, A. 2021. HyperExtended Light-Face: A Facial Attribute Analysis Framework. In *ICEET*.
- Terhorst, P.; Kolf, J. N.; Damer, N.; Kirchbuchner, F.; and Kuijper, A. 2020. SER-FIQ: Unsupervised estimation of face image quality based on stochastic embedding robustness. In *CVPR*.
- Tölle, M.; Köthe, U.; André, F.; Meder, B.; and Engelhardt, S. 2022. Content-Aware Differential Privacy with Conditional Invertible Neural Networks. In *DeCaF*. Springer.
- Voigt, P.; and Von dem Bussche, A. 2017. The eu general data protection regulation (gdpr). *A Practical Guide, 1st Ed*.
- Wang, J.; Sun, K.; Cheng, T.; Jiang, B.; Deng, C.; Zhao, Y.; Liu, D.; Mu, Y.; Tan, M.; Wang, X.; Liu, W.; and Xiao, B. 2021. Deep High-Resolution Representation Learning for Visual Recognition. *TPAMI*, 43(10).
- Wang, T.-C.; Liu, M.-Y.; Zhu, J.-Y.; Tao, A.; Kautz, J.; and Catanzaro, B. 2018. High-Resolution Image Synthesis and Semantic Manipulation with Conditional GANs. In *CVPR*.
- Wang, Y.; Si, C.; and Wu, X. 2015. Regression model fitting under differential privacy and model inversion attack. In *IJCAI*.
- Wen, Y.; Liu, B.; Ding, M.; Xie, R.; and Song, L. 2022. Identitydp: Differential private identification protection for face images. *Neurocomputing*, 501.
- Wen, Z.; Lin, W.; Wang, T.; and Xu, G. 2021. Distract your attention: multi-head cross attention network for facial expression recognition. *arXiv:2109.07270*.
- Westerlund, M. 2019. The emergence of deepfake technology: A review. *TIM Review*, 9(11).
- Wu, W.; Qian, C.; Yang, S.; Wang, Q.; Cai, Y.; and Zhou, Q. 2018. Look at Boundary: A Boundary-Aware Face Alignment Algorithm. In *CVPR*.
- Xu, Y.; Deng, B.; Wang, J.; Jing, Y.; Pan, J.; and He, S. 2022. High-resolution face swapping via latent semantics disentanglement. In *CVPR*.
- Yu, J.; Xue, H.; Liu, B.; Wang, Y.; Zhu, S.; and Ding, M. 2020. Gan-based differential private image privacy protection framework for the internet of multimedia things. *Sensors*, 21(1).
- Zhang, X.; Park, S.; Beeler, T.; Bradley, D.; Tang, S.; and Hilliges, O. 2020. ETH-XGaze: A Large Scale Dataset for Gaze Estimation under Extreme Head Pose and Gaze Variation. In *ECCV*.
- Zhou, J.; and Pun, C.-M. 2020. Personal privacy protection via irrelevant faces tracking and pixelation in video live streaming. *TIFS*, 16.
- Zhou, Y.; and Gregson, J. 2020. Whenet: Real-time fine-grained estimation for wide range head pose. *arXiv:2005.10353*.
- Zhu, Y.; Li, Q.; Wang, J.; Xu, C.-Z.; and Sun, Z. 2021. One shot face swapping on megapixels. In *CVPR*.

Disguise without Disruption: Utility-Preserving Face De-Identification (Supplementary Material)

Summary

In this supplementary material, we augment the main paper in the following aspects:

- We provide comprehensive implementation details of our framework *Disguise*;
- We conduct additional ablation studies covering various variations of our methods;
- We include extra qualitative comparisons with other techniques using images in real-world scenarios, encompassing medical settings and images containing multiple faces.

Further Implementation Details

Architecture. We build our face-swapping model g based on the architecture and training framework proposed in Sim-Swap (Chen et al. 2020). The identity-merging module uses a MLP_{θ_z} with two layers and feature sizes of [1024, 1024, 512]. The identity-transforming MLP_{θ_z} , on the other hand, is a 3-layer network with feature sizes [512, 2048, 1024, 512]. The VED encoder consists of two dense layers of sizes [512, 1024, 1024], followed by two parallel layers of size [512] to predict the mean and variance in latent space. The VED decoder has three dense layers of sizes [512, 1024, 1024, 512]. We use tanh as final activation throughout the model.

Training. We apply the Adam optimizer (Kingma and Ba 2014) with $\beta_1 = 0$ and $\beta_2 = 0.999$, learning rate 10^{-4} , and a batch size of 4. We train our pipeline in two stages: (1) we first pre-train the face-swapper g according to (Chen et al. 2020) for 1M iterations; (2) then we fine-tune it together with utility module and ID transformer for another 100k iterations. This is illustrated in Figure 6.

Evaluation. For the de-correlation evaluation presented in Figure 5(e), the MLP attacker networks consist of three layers of feature sizes [512, 2048, 1024, 512], tasked to reconstruct the original identity embedding from the obfuscated one extracted from the edited image. We train one attacker specific to each obfuscation method (CIAGAN (Maximov, Elezi, and Leal-Taixé 2020), DeepPrivacy (Hukkelås, Mester, and Lindseth 2019), ours, *etc.*). We use Adam optimizer with a learning rate of 10^{-3} and a total epoch of 100 epochs. We trained the decoders on CelebA-HQ and evaluated them on LFW.

More Ablation Studies and Analyses

Complementing Ablation Study section in the main paper, we delve deeper into assessing how diverse ID extraction methods, ID transformation techniques, and utility experts can collectively influence the overall obfuscation pipeline.

Impact of ID extraction models. Existing face swapping solutions (Chen et al. 2020) also leverage out-of-the-box identification networks (*e.g.*, ArcFace (Deng et al. 2019) as the most common choice), but they do not provide any analysis on the possible bias that these pretrained methods may have and how such bias may impact the de-identification process, *e.g.*, by improperly disentangling some facial features.

To address this concern, we present our analyses in Tables 6, 7, and 8. Our method can harness multiple ID extractors, thus we compare distinct versions of our solutions: employing ArcFace (Deng et al. 2019), AdaFace (Kim, Jain, and Liu 2022), SphereFace (Liu et al. 2017), or a fusion of these methods. Notably, we exclude the assessment on one ID extractor when it is utilized in the de-identification pipeline, *e.g.* AdaFace in Table 6 last two rows and SphereFace in Table 8 last two rows, ensuring fairness.

Table 8 underscores that combining various ID extractors yields enhanced de-identification and non-invertibility. Particularly with AdaFace-based pipelines, this effect is evident. When solely used, AdaFace exhibits slight bias or performance limitations (*vis-à-vis* FaceNet (Schroff, Kalenichenko, and Philbin 2015) or SphereFace (Liu et al. 2017) for re-identification), possibly due to missing biometric features, leading to higher re-identification rates post-obfuscation compared to other ID extractors. However, coupling AdaFace with an alternative ID method like ArcFace (Deng et al. 2019) mitigates the re-identification rate effectively. Moreover, combining multiple identity extractors notably boosts resilience against inversion attacks (as evident in the last two columns of Table 8), as anticipated from mixture-of-experts approaches.

Nonetheless, a trade-off between preserving privacy and utility remains observable. As Table 7 illustrates, solutions leveraging multiple ID extractors tend to exert a slightly greater impact on utility attributes, resulting in a minor accuracy dip for the designated downstream tasks. Navigating this trade-off and devising a solution that better disentangles identity and utility attributes—given their non-overlapping nature—remains an open challenge. Nevertheless, we believe that *Disguise* represents a substantial stride forward in this regard (as evident from comparisons to state-of-the-art in both the main paper and this document).

Impact of ID transformation models. Figure 7 extends the analysis presented in Tables 4 and 5, highlighting the superiority of our VED-based obfuscation scheme compared to the other MLP-based proposed solution, as well as their superiority compared to prior art. The first row in Figure 7 shows that compared to other methods, our VED-based model is further from the positive pairs both on the histogram and ROC curve, demonstrating the best de-identification abil-

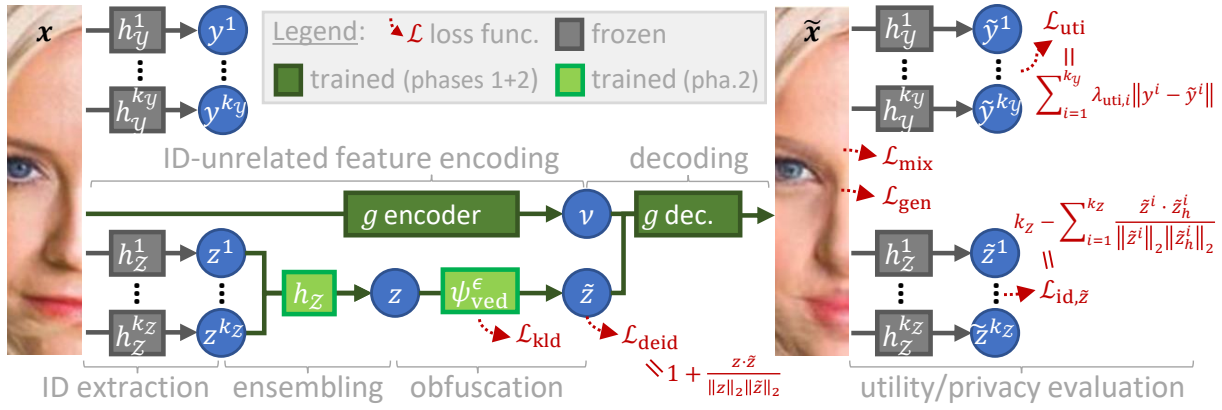


Figure 6: Detailed training pipeline of *Disguise*, in supplement to Figure 2. The proposed solution is end-to-end differentiable. However, in practice, to guide the optimization process, we train the network in two phases. Firstly, we train the face-swapping network (the branch marked in dark green); then in the second phase, we add the ID obfuscation branch (marked in light green) and the utility-guaranteeing module (the branch on top) to finetune the whole network.

Table 6: Identification / validation rate (\downarrow , lower = better) and image quality evaluation (\uparrow , higher = better) over edited LFW data.

Methods	TPR (%) @ FPR= 10^{-3} / Accuracy (%) \downarrow				FIQ \uparrow SER
	FaceNet	SphereFace	AdaFace	Average	
Original	93.83 / 97.1	87.90 / 96.2	95.43 / 97.7	92.39 / 97.0	0.77
Ours (arc, opp, \emptyset)	0.63 / 51.5	0.03 / 50.0	0.03 / 50.0	0.23 / 50.5	0.81
Ours (arc, ved, emo)	0.23 / 50.1	0.00 / 50.0	0.07 / 50.0	0.10 / 50.0	0.90
Ours (arc, ved, eye)	0.03 / 50.0	0.03 / 50.0	0.00 / 50.0	0.02 / 50.0	0.90
Ours (arc, mlp, emo)	0.03 / 50.0	0.00 / 50.0	0.03 / 50.0	0.02 / 50.0	0.90
Ours (arc, mlp, eye)	0.00 / 50.0	0.00 / 50.0	0.03 / 50.0	0.01 / 50.0	0.90
Ours (arc, mlp, mix)	0.00 / 50.0	0.00 / 50.0	0.03 / 50.0	0.01 / 50.0	0.90
Ours (ada, mlp, eye)	3.73 / 70.8	0.43 / 65.5	NA (c.f. train/ eval overlap)	2.08 / 68.2	0.87
Ours (mix, mlp, eye)	0.07 / 50.0	0.00 / 50.0		0.04 / 50.0	0.91

ity. The second row shows that when we introduce more β noise in our MLP model, both the histogram and ROC curve move closer towards the positive pairs. When $\beta = 0.5$, our MLP model can de-identify facial images on which recognition model has performance close to random guess. For our VED model, when increasing the α noise, the histogram stays close to the negative pairs and the ROC curve stays close to the diagonal line, as shown in the third row. These results suggest that our VED model achieves the best de-identification while ensuring non re-identifiability.

As a reminder, we define α and β as inversely proportional to ϵ , c.f. $\alpha = \frac{\Delta\psi}{\epsilon}$ and $\beta = \frac{\Delta\psi_{\text{mlp}}}{\epsilon}$. As a measure of privacy budget, the higher ϵ is fixed (i.e., the lower α or β), the higher the privacy loss, c.f. $\log P(\tilde{z}|z) - \log P(\tilde{z}|z') \leq \epsilon$ according to the formal definition in Problem Formulation subsection. Local differential privacy (LDP) guarantees that an adversary observing \tilde{z} cannot determine with some degree of confidence if it comes from z or z' . E.g., $\epsilon = 0$ would mean zero confidence in linking a masked ID to a specific input one, as only noise would be transferred (c.f. Laplacian noise with $\alpha = \frac{\Delta\psi}{\epsilon} = \infty$). To choose ϵ (and thus α) adequately based on privacy budget, one should first estimate the sensitivity Δ of the processing function. Following stan-

dard practice (Liu et al. 2021; Wen et al. 2022), we measure the sensitivity of ours empirically: e.g., over LFW dataset, we obtain $\Delta\psi_{\text{ved}} = \sup_{z,z'} \|\psi(z) - \psi(z')\|_1 = 33.92$ (e.g., hence fixing $\alpha = 2$ means opting for a relative privacy budget equals to $\epsilon = 67.84$).

We enhance the analysis presented in Table 5 with additional insights from Table 9. This new table illustrates the performance of the ID transformation scheme, which entails applying solely ϵ -controlled Laplace noise to the features without employing additional neural networks for further vector obfuscation. Comparatively, our proposed Multi-Layer Perceptron (MLP) and Variational Encoder-Decoder (VED) solutions distinctly elevate identity obfuscation beyond the effects of noise-only feature manipulation, as depicted in Table 9. However, their continuous nature renders them more susceptible to re-identification risk, especially for similar privacy budgets. In cases of slight noise values, they could inadvertently map distinct inputs to a common fabricated identity. Despite this, we maintain the conviction that our VED-based approach strikes the most optimal balance between maximal de-identification and non-reidentifiability.

Comparison with other noise-based ID tampering methods. Some other methods (Li and Lin 2019; Liu et al. 2021;

Table 7: Utility performance comparison of different versions of our methods over diverse downstream tasks on LFW dataset (Huang et al. 2008).

Methods	Facial landmarks (L2 pixel distance ↓)								Gaze estimation (MAE ° ↓)				Emotion (Accuracy % ↑)	
	RetinaFace (5 points)				Dlib (68 points)				L2CS Net		ETH XGaze		(Accuracy % ↑)	
	All	Eyes	Nose	Mouth	All	Eyes	Nose	Mouth	Pitch	Yaw	Pitch	Yaw	DAN	DF
Ours (arc, opp, \emptyset)	12.5	7.6	5.4	8.0	177.6	25.8	16.1	49.8	7.0	9.2	6.1	12.1	51.2	50.5
Ours (arc, ved, emo)	12.7	7.6	5.7	8.1	187.6	26.5	18.8	55.6	7.4	10.8	6.1	13.1	58.8	49.8
Ours (arc, ved, eye)	12.9	7.7	5.6	8.2	203.3	28.8	19.8	60.0	6.8	8.4	5.6	10.0	46.2	47.0
Ours (arc, mlp, emo)	17.1	10.3	7.6	10.8	210.9	31.1	20.3	62.3	7.4	11.3	6.4	14.2	59.5	51.0
Ours (arc, mlp, eye)	17.3	10.4	7.6	11.2	218.1	31.2	20.1	63.1	7.0	8.0	5.9	9.9	42.9	46.9
Ours (arc, mlp, mix)	16.5	9.9	7.3	10.6	202.4	28.3	18.5	61.4	6.9	7.8	5.5	9.6	59.5	49.2
Ours (arc, mlp, eye)	17.3	10.4	7.6	11.2	218.1	31.2	20.1	63.1	7.0	8.0	5.9	9.9	42.9	46.9
Ours (ada, mlp, eye)	15.9	9.3	7.3	10.1	211.4	30.2	21.9	64.9	6.3	7.3	5.4	9.2	43.8	46.8
Ours (sph, mlp, eye)	14.9	8.9	6.5	9.5	205.2	28.7	21.2	60.5	6.1	7.5	5.4	10.3	47.4	49.4
Ours (arc+ada, mlp, eye)	15.7	9.3	6.9	10.3	202.8	27.0	18.7	62.1	7.2	7.8	6.2	9.7	42.8	46.9
Ours (arc+sph, mlp, eye)	19.7	11.7	8.4	12.8	230.1	34.0	22.7	66.0	6.8	7.4	5.8	9.0	39.1	45.9

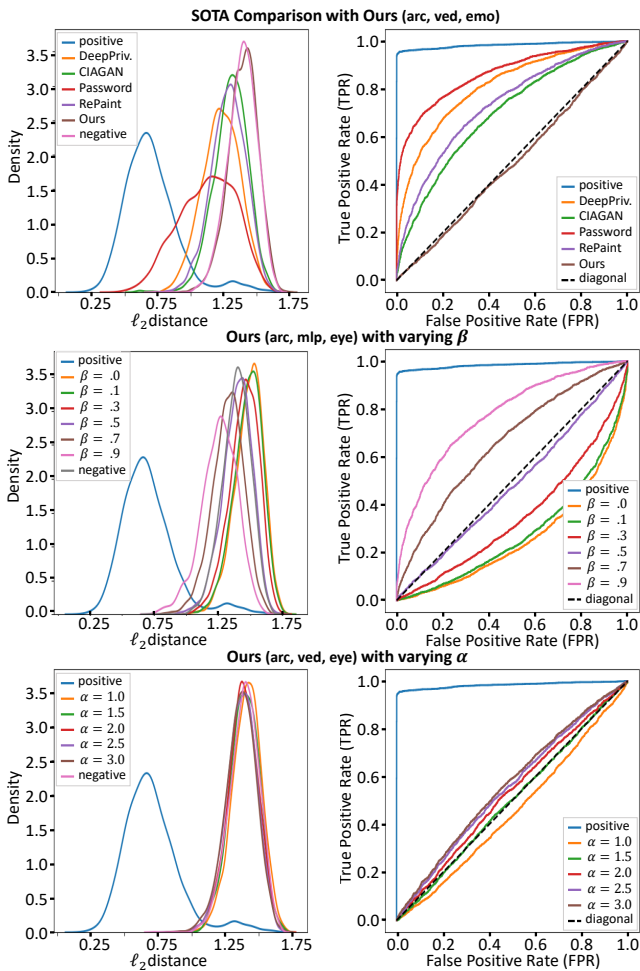


Figure 7: Left: Histogram of ℓ_2 distances between positive, negative, and original-anonymized pairs from LFW set. Right: ROC curves of validation rate for images altered by various methods.

Table 8: Re-identification performance and invertibility of different proposed ID transformation methods. (mix1 indicates arc+ada, mix2 indicates arc+sph.)

Methods	TPR (%) @ FPR=1e-3 ↓			
	Swapped		Inverted	
	FaceNet	SphereFace	FaceNet	SphereFace
Ours (arc, mlp, eye)	0.00	0.00	52.90	45.97
Ours (ada, mlp, eye)	3.73	0.43	49.77	42.63
Ours (mix1, mlp, eye)	0.07	0.00	36.70	34.70
Ours (sph, mlp, eye)	0.00	NA	68.70	NA
Ours (mix2, mlp, eye)	0.00	NA	31.93	NA

Table 9: Evaluation of ID transformation based on noise application only, in terms of de-identification and non-invertibility of the resulting images.

Methods		TPR (%) @ FPR=1e-3 ↓			
Net.	Noise	Swapped		Inverted	
		FaceNet	SphereFace	FaceNet	SphereFace
∅	$\beta = 0.25$	19.27	12.87	1.27	0.30
	$\beta = 0.5$	15.37	9.90	1.37	0.30
	$\beta = 1.0$	13.03	7.73	1.47	0.43
	$\beta = 2.0$	12.63	6.23	1.93	0.57
	$\beta = 4.0$	11.30	6.50	1.47	0.47
	$\beta = 8.0$	11.30	6.27	2.23	0.50

Li and Clifton 2021; Wen et al. 2022), have been recently proposed to tackle de-identification of facial images by extracting identity features from the target data, altering it, and decoding it back into a similar but obfuscated image. While we could not satisfyingly reproduce their results (no implementation has been released), we could approximate their solution using our own framework. Indeed, most of these methods can be described as a subset of our modular solution, *i.e.*, minus our main contributions. This is especially true for DP-Image (Liu et al. 2021) (not peer-reviewed yet) and IdentityDP (Wen et al. 2022) (published in August, the 28th, 2022), which use an image encoder-decoder combined with an ID extractor (Deng et al. 2019) and ID/image feature mixer, similar to ours. However, they do not provide our additional guarantees in terms of disentanglement of the

facial attributes and preservation of the utility ones by using mixture-of-experts supervision. More importantly, they obfuscate the extracted ID vector (before injecting it with the residual image features and decoding it back into an image) only by adding Laplace noise to them. They do not leverage additional transformations in the ID latent space to ensure optimal de-identification, such as our MLP and VED neural functions.

To highlight the impact of our proposed ID transformation functions and indirectly compare to these other solutions, we direct the readers to Figure 8. For each original image, we display the results obtained by transforming the extracted ID features either after only adding Laplace-based noise to them (first row); after applying our proposed $\psi_{\text{mlp}}^\epsilon$, *i.e.*, adding Laplace noise and then passing the vector to our MLP optimized to ensure de-identification (second row); or after passing the vector to our VED $\psi_{\text{ved}}^\epsilon$, which also applies ϵ -controlled noise to the data in its own latent space (third row). For each solution, we provide several results with different privacy budgets (β parameter, encompassing ϵ).

We observe that applying only ϵ -controlled noise to the ID vector results in images barely obfuscated (*e.g.*, same nose/cheek/eyebrow shapes) compared to additionally using our proposed neural functions, for the same privacy budgets β . Furthermore, our VED-based solution provides better continuity in the obfuscated results w.r.t. β compared to the other two variants. Such continuity makes choosing an adequate privacy budget much more intuitive and straightforward for users.

Impact of utility experts. Our observations indicate that engaging in fine-tuning alongside utility experts yields notable enhancements in preserving performance for downstream tasks, as evidenced by the findings in Tables 6 and 7. To delve into specifics, we note that in the gaze estimation task, the model fine-tuned with the inclusion of eye-related utility experts showcases the most minimal offset, denoting superior alignment. Similarly, the same pattern emerges in the context of emotion recognition, where the model fine-tuned with emotion-centric utility experts achieves optimal results. On the other hand, concerning facial landmarks, intriguing dynamics come to light. The model deprived of fine-tuning with emotion or gaze experts demonstrates the highest performance in this regard. This contrast highlights the existence of a trade-off phenomenon, indicating that distinct utility experts exert varying degrees of influence, necessitating a balanced consideration.

More Qualitative Evaluation and Comparisons

In this section, we provide additional qualitative results highlighting the quality of privacy and utility preservation provided by the proposed method, compared to the most popular face anonymization methods, such as blurring (Frome et al. 2009), pixelation (Zhou and Pun 2020), Password (Gu et al. 2020), CIAGAN (Maximov, Elezi, and Leal-Taixé 2020), DeepPrivacy (Hukkelås, Mester, and Lindseth 2019), and Repaint (Lugmayr et al. 2022). We also exhibit the ability to directly run on images in the wild without the need of complex post-preprocessing, in contrast to (Li and

Clifton 2021; Barattin et al. 2023).

More qualitative comparisons on LFW. Figure 9 complements Figure 4 with more comparisons. Simpler methods, such as blurring and pixelation, provide effective anonymization, but the resulting facial images cannot be leveraged for downstream tasks. For the other deep-learning-based solutions, the observations are similar to those made w.r.t. Figure 4. Password (Gu et al. 2020) fails at removing identifying features; whereas RePaint (Lugmayr et al. 2022) has difficulties hallucinating entire new faces, resulting in images too distorted to be useful. CIAGAN (Maximov, Elezi, and Leal-Taixé 2020) and DeepPrivacy (Hukkelås, Mester, and Lindseth 2019) provide strong anonymization and pseudo-realistic results, but they still suffer from artifacts that can also impair usability (in terms of saliency and utility attributes). Our method sometimes struggles with out-of-distribution images (*e.g.*, facial images with lighting conditions hiding key features) causing some utility loss, but it overall yields realistic images sharing utility attributes with the original ones while successfully altering identifying traits (nose width, thickness of the eyebrows, shape of cheeks, *etc.*).

Sensitive images taken in medical settings. Closer to the target use-cases discussed in the Introduction, we also share additional results on sensitive images taken in medical settings (the images were taken, edited, and shared with the consent of the depicted volunteers), *c.f.* Figure 10. Once again, we note the superiority of the proposed method in terms of image quality and usability. For example, the gaze and facial expression are better preserved, and so are elements occluding the faces (oxygen mask, glasses). If the obfuscated data were to be used for training algorithms on face-focused tasks for medical environments, preserving such challenging non-facial features would be important to ensure the robustness of these methods after deployment.

Group photos with multiple faces. Figure 11 shows some results when applying the evaluated methods to group images, again highlighting the performance of our method compared to the state-of-the-art. *E.g.*, while DeepPrivacy is able to generate high-quality *fake* faces, it does not preserve key utility attributes as well as our method (*e.g.*, changing gaze directions or facial expressions, adding glasses, *etc.*).

Note that for such group images or images showing more than just a face (*c.f.* Figure 11), we first apply InsightFace (noa 2022; Deng et al. 2019), a face detection model, to obtain the region for each face present in the image; then we apply the de-identification methods to each corresponding crop separately; before merging everything back into the obfuscated image.

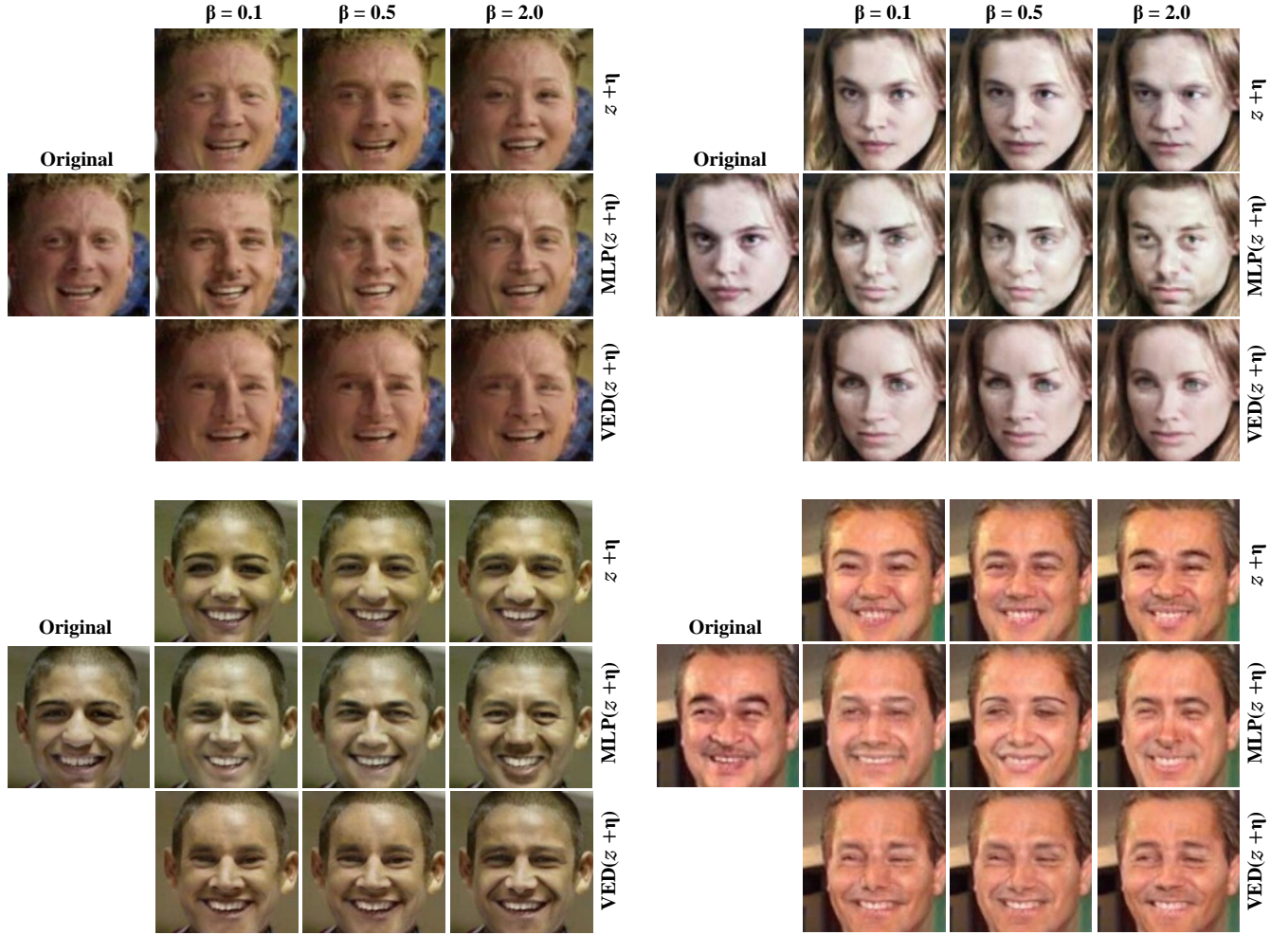


Figure 8: Comparison of different ID transformation functions in terms of their impact on the resulting obfuscated images. We compare (1) applying only Laplace noise to the extracted ID vectors (noted “ $z + \eta$ ” in the figure), (2) applying our proposed $\psi_{\text{mlp}}^\epsilon$, *i.e.*, applying noise and our MLP (noted “ $\text{MLP}(z + \eta)$ ”), or (3) applying our $\psi_{\text{ved}}^\epsilon$, *i.e.*, applying noise and our VED (noted “ $\text{VED}(z + \eta)$ ” here).

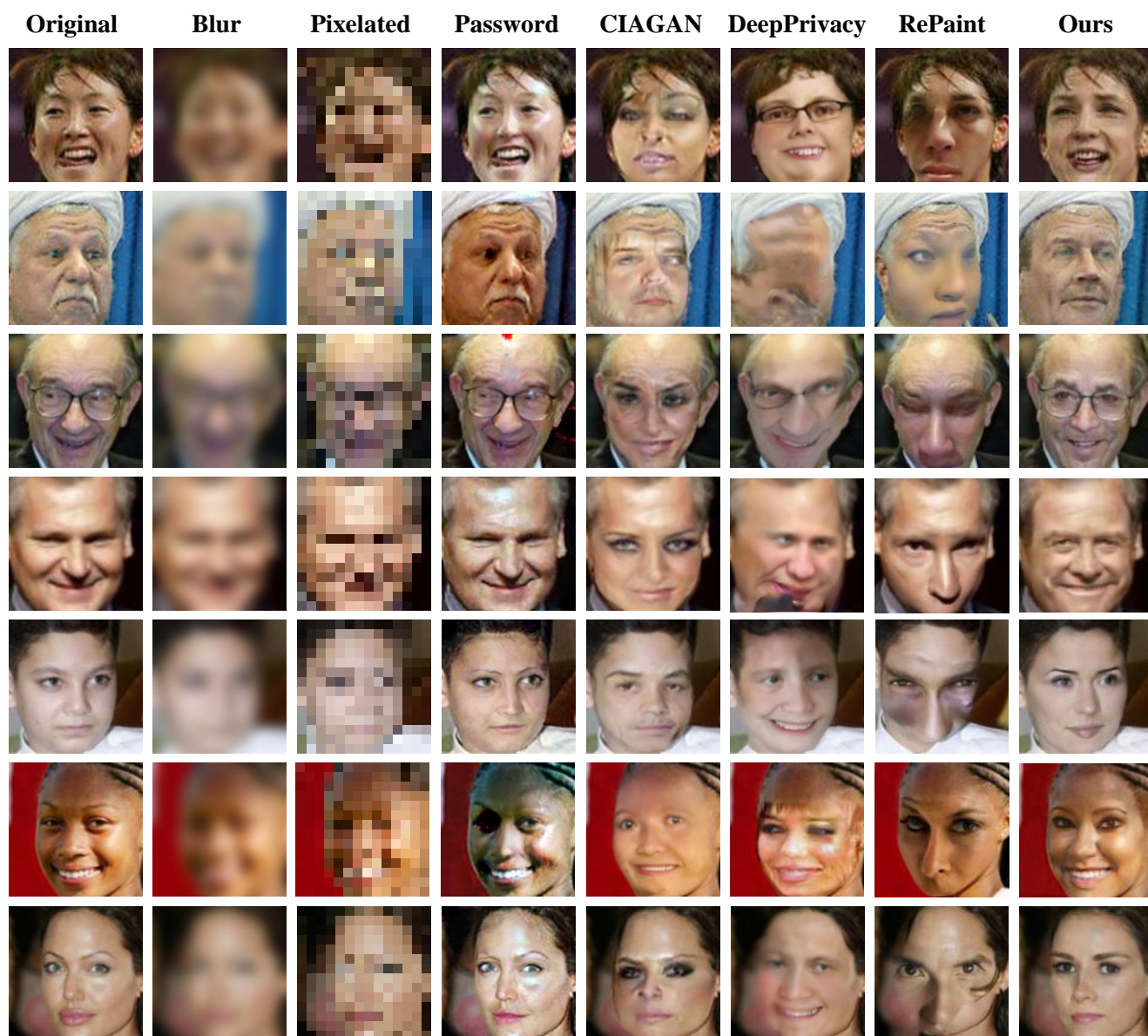


Figure 9: Qualitative results of face anonymization methods. Our method anonymizes images while maintaining utility and image quality.

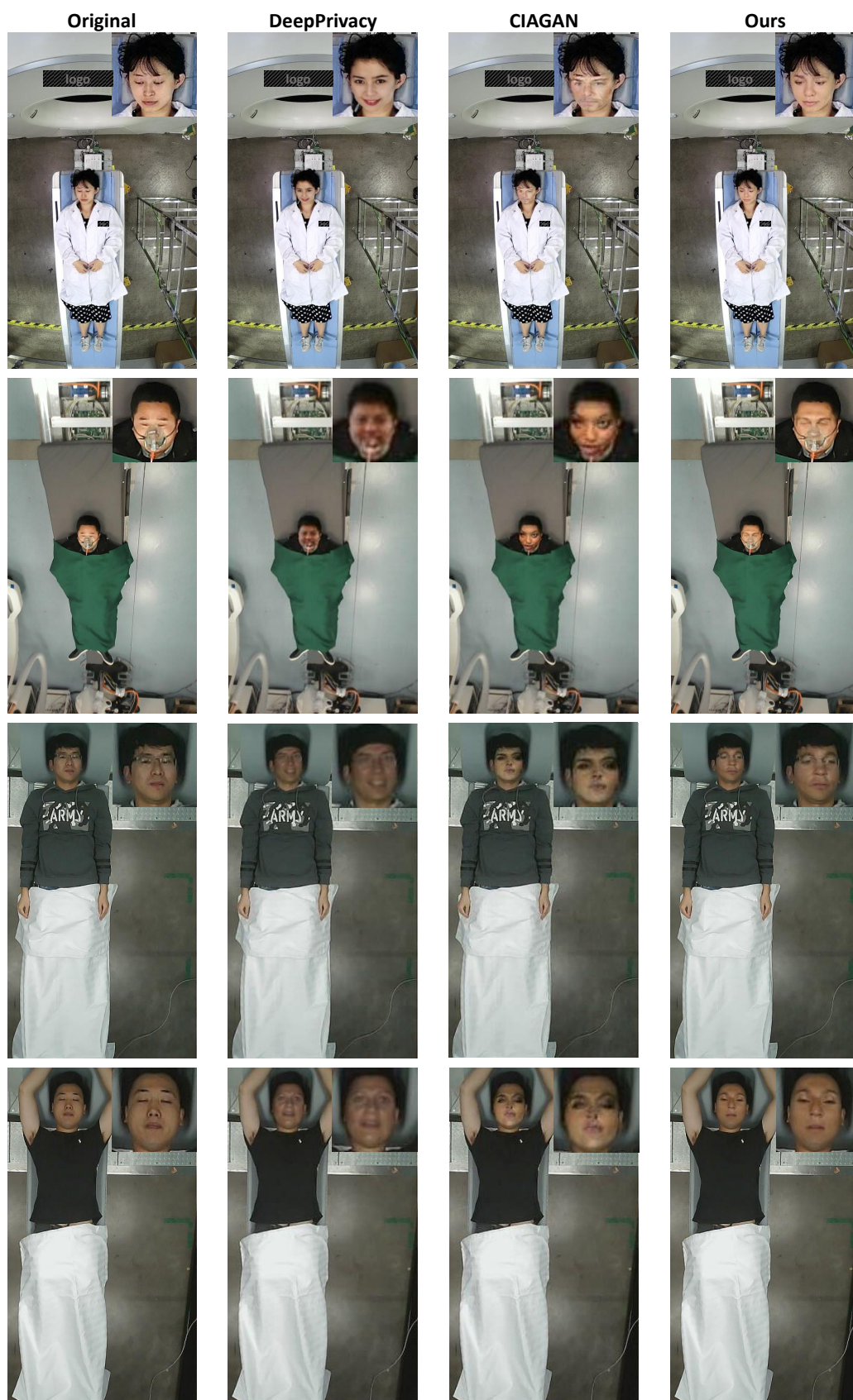


Figure 10: Qualitative results of face anonymization methods on images collected in medical settings.



Figure 11: Qualitative results of face anonymization methods on images depicting multiple persons.